MODE II FATIGUE CRACK GROWTH IN ALUMINUM ALLOYS AND MILD STEEL

A. Otsuka, K. Mori, T. Ohshima and S. Tsuyama

Department of Iron & Steel Engineering, Nagoya University
Nagoya 464, Japan

ABSTRACT

Mode II fatigue crack growth behavior has been investigated on 7075-T6 and 2017-T4 aluminum alloys and annealed mild steel. Aluminum alloys show mode II growth in the range of larger ΔK_{II} than some critical values. On mild steel, mode II growth is seen in the narrow region of smaller ΔK_{II} than a critical value, whereas in the region where ΔK_{II} is larger than this critical value, tensile mode growth occurs. It is found that mode II growth in annealed mild steel is fractographically similar to the stage I in the initial stage of fatigue crack growth.

KEYWORDS

Mode II growth; mode II loading; ΔK-threshold; fatigue crack growth; stage I growth.

INTRODUCTION

Mode II loading or shear loading sometimes occurs in various components of actual structures. Therefore, it would be important to clarify the behavior of fatigue crack growth under mode II loading not only from the fundamental interest concerned with the mechanism of fatigue crack growth but also from practical view point. Some investigations (Roberts and Kibler, 1971; Otsuka, Mori, and Miyata, 1975; Otsuka and co-workers, 1979; Yokobori, Yokobori, and Kamei, 1977; Pook, 1977; Pook and Greenan, 1979) have been made on this subject, but it is not yet clear in many respects. According to the previous report (Otsuka, Mori, and Miyata, 1975), two modes of fatigue crack growth, mode II growth and tensile mode growth, are sometimes observed under mode II loading. Based on this result, the emphasis of this research has been placed on obtaining the ΔK_{IIth}, the lower limiting value of ΔK_{II} for fatigue crack growth under mode II loading, for each of these two modes of fatigue crack growth. The relation between the fatigue crack growth under mode II loading and that under mode I loading has also been considered. The loading condition used in this research, repeated mode II loading (ΔK_{II}) superimposed by static $K_I(K_{IS})$, has been selected for the reason that it will be the one to be occasionally encountered during actual service.

MATERIALS AND EXPERIMENTAL PROCEDURES

Tests were made on 7075-T6 and 2017-T4 aluminum alloys and annealed mild steel.

TABLE 1 Chemical Composition, %

Steel	C	Si	Mn	P	S
Mild Steel(JIS SPCC)	0.07	0.02	0.35	0.012	0.015

Aluminum Alloy	Si	Fe	Cu	Mn	Mg	Cr	Zn	Ti
7075	0.07	0.29	1.60	0.05	2.70	0.20	5.36	0.06
2017	0.62	0.33	4.14	0.58	0.62	0.03	0.12	-

TABLE 2 Heat Treatments and Mechanical Properties

Materials	Heat Treatment	ASTM G.S.No.	Yield Stress (MPa)	U.T.S. (MPa)	Elongation (%)
Mild Steel (JIS SPCC)	950°C, 3h Furnaced Cooled	5.5	159	285	65.6
7075	T6	-	516*	587	9.4
2017	T4	-	288*	469	25.5

* 0.2% Offset Stress

Their chemical compositions and mechanical properties are shown in Tables 1 and 2. Specimen and testing apparatus used for mode II loading tests are shown in Figs. 1 and 2, respectively. Mode II fatigue crack growth tests were carried out in the range in which the fatigue crack growth is limited to the central 50% of the specimen width where the distribution of shearing stress τ is almost uniform. The calculation of ΔK_{II} was made by the formula $K_{II} = \tau\sqrt{\pi a}$ where τ is the uniform shearing stress in the central 50% of the specimen width. According to the measured results, τ above mentioned is given by $\tau = 1.4\tau_{mean}$, where τ_{mean} is applied shearing force divided by the gross-section area of the specimen. Tests were made under combined repeated K_{II} (ΔK_{II}) and constant K_I (K_{IS}) loading, where ΔK_{II} was applied by alternating shear, namely $K_{IImax} = K_{II}$ and $K_{IImin} = -K_{II}$.

RESULTS AND DISCUSSION

7075-T6 : Figure 3 shows the experimental results on the fatigue crack growth behavior of 7075-T6 specimens under ΔK_{II} superimposed by K_{IS}. ΔK_{IIth}(mode II) and ΔK_{IIth}(tensile mode), threshold value of ΔK_{II} for mode II growth and that for tensile mode growth, respectively, are obtained by ΔK_{II}-decreasing tests. 7075-T6 specimens show mode II growth in the plane of precrack where ΔK_{II} is larger than ΔK_{IIth}(mode II) shown in Fig. 3, and they show tensile mode growth when ΔK_{II} is reduced beyond ΔK_{IIth}(mode II). In the region ΔK_{II} is smaller than ΔK_{IIth}(tensile mode), fatigue crack growth does not occur. Experimental data in Fig. 4 show the ΔK_{II} versus da/dN relation for mode II growth. It is seen that the ΔK_{II} versus da/dN relation is almost independent of K_{IS}. The dash-dot-line in Fig. 4 shows the ΔK_I versus da/dN relation obtained from usual mode I fatigue data. The dashed line in Fig. 4 and the curve of ΔK_{IIth}(tensile mode) in Fig. 3 were obtained by the calculation based on the ΔK_I versus da/dN relation shown in Fig. 4 in the following way.

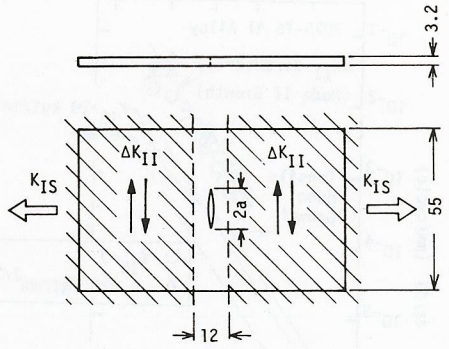

Fig. 1 Mode II specimen.

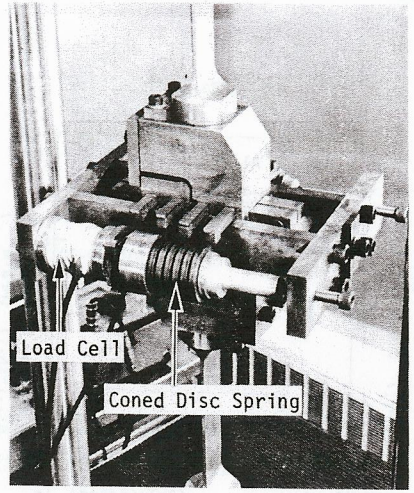

Fig. 2 Mode II loading apparatus.

The maximum and minimum values of the local tensile stress near the tip of the crack subjected to combined ΔK_{II} (= $2K_{II}$, stress ratio R = -1) and K_{IS} are given by the following formula,

$$\sigma_{r\theta,max} = \frac{1}{\sqrt{2\pi r}} \cos\frac{\theta}{2} \left[K_{IS} \cos^2\frac{\theta}{2} + \frac{3}{2} K_{II} \sin\theta\right] \quad (1)$$

$$\sigma_{r\theta,min} = \frac{1}{\sqrt{2\pi r}} \cos\frac{\theta}{2} \left[K_{IS} \cos^2\frac{\theta}{2} - \frac{3}{2} K_{II} \sin\theta\right] \quad (2)$$

To define the tensile stress distribution around the crack tip instead of the stress at a particular point, we use the parameter $K_\sigma = \sqrt{2\pi r}\cdot\sigma_{r\theta}$. Here we assume that tensile mode growth depends on the positive part of the range of K_σ, $\Delta K_\sigma = K_{\sigma,max} - K_{\sigma,min}$, in case $K_{\sigma,min} \geqq 0$, and $\Delta K_\sigma = K_{\sigma,max}$ in case $K_{\sigma,min} < 0$. ΔK_σ's defined as above are given by the following formula.

$$\Delta K_\sigma = 3K_{II} \cos\frac{\theta}{2} \sin\theta \ , \qquad K_{\sigma,min} \geq 0 \quad (3)$$

$$\Delta K_\sigma = K_{IS} \cos^3\frac{\theta}{2} + \frac{3}{2} K_{II} \cos\frac{\theta}{2} \sin\theta \ , \qquad K_{\sigma,min} < 0 \quad (4)$$

ΔK_σ's given by the Eqs. (3) and (4) take the maximum value with respect to θ, $\Delta K_{\sigma,max}$ as shown by Eqs. (5), (6), and (7) at particular values of θ given by Eqs. (8), (9), and (10) depending on the value of K_{IS}/K_{II}.

$$\Delta K_{\sigma,max} = \cos\frac{\theta_m}{2} \left[K_{IS} \cos^2\frac{\theta_m}{2} + \frac{3}{2} K_{II} \sin\theta_m\right] , \qquad K_{IS}/K_{II} \leqq 1.34 \quad (5)$$

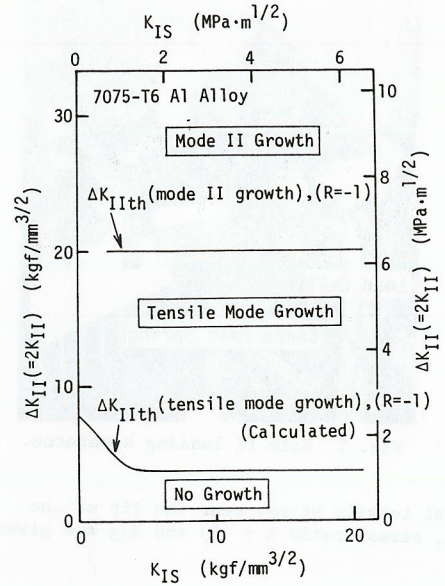

Fig. 3 Fatigue crack growth behavior under mode II loading in 7075-T6 aluminum alloy (Otsuka, Mori, Ohshima, and Tsuyama, 1979).

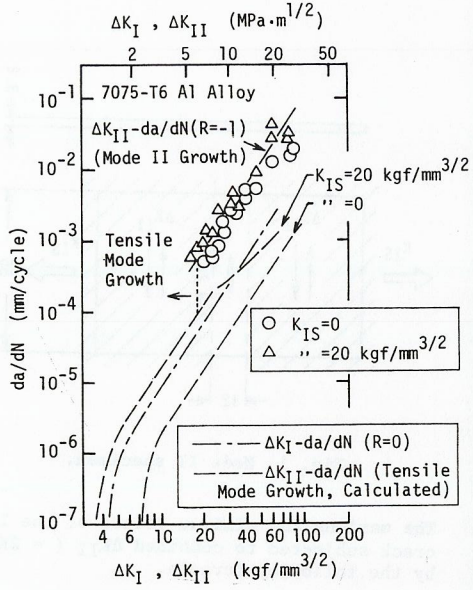

Fig. 4 ΔK_{II} versus da/dN under mode II loading for 7075-T6 aluminum alloy. Dashed lines show ΔK_{II} versus da/dN for tensile mode growth obtained by calculation.

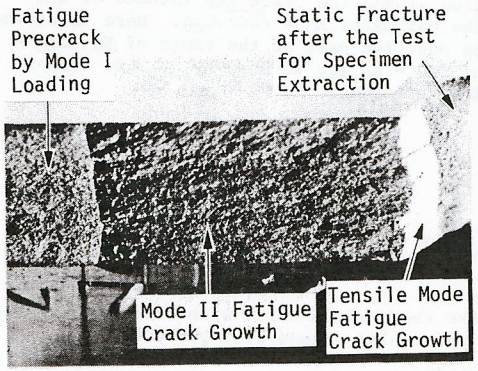

Fig. 5 Macroscopic appearance of mode II and tensile mode fatigue crack growth under mode II loading in 7075-T6 aluminum alloy.

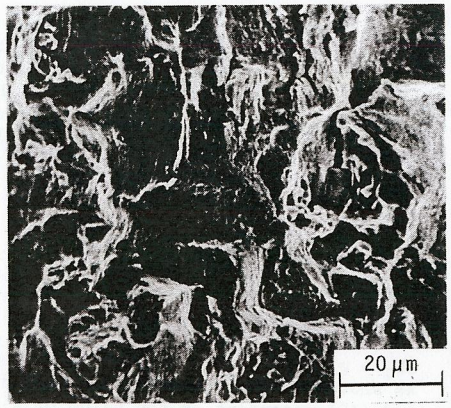

Fig. 6 An example of SEM fractograph of mode II fatigue crack growth. ΔK_{II} = 26.2kgf/mm$^{3/2}$(8.1MPa·m$^{1/2}$, K_{IS} = 20kgf/mm$^{3/2}$(6.2MPa·m$^{1/2}$) da/dN = 1.5 x 10^{-3}mm/cycle

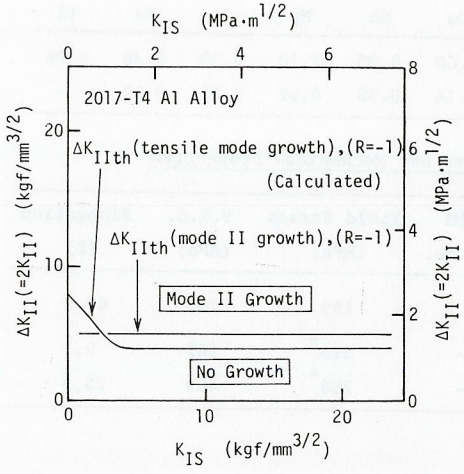

Fig. 7 Fatigue crack growth behavior under mode II loading in 2017-T4 aluminum alloy (Otsuka, Mori, Ohshima, and Tsuyama, 1979).

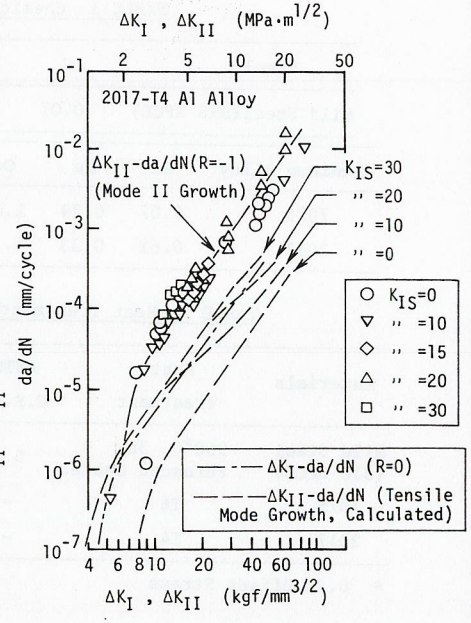

Fig. 8 ΔK_{II} versus da/dN under mode II loading for 2017-T4 aluminum alloy. Dashed lines show ΔK_{II} versus da/dN for tensile mode growth obtained by calculation.

$$\Delta K_{\sigma,max} = \cos\frac{\theta_o}{2}\left[K_{IS}\cos^2\frac{\theta_o}{2} + \frac{3}{2}K_{II}\sin\theta_o\right], \quad 1.34 < K_{IS}/K_{II} \leqq 2.12 \qquad (6)$$

$$\Delta K_{\sigma,max} = 3K_{II}\cos\frac{\theta_n}{2}\sin\theta_n, \qquad K_{IS}/K_{II} > 2.12 \qquad (7)$$

where $$\theta_m = 2\tan^{-1}\frac{1}{4}\left[\sqrt{(K_{IS}/K_{II})^2 + 8} - K_{IS}/K_{II}\right] \qquad (8)$$

$$\theta_o = 2\tan^{-1}\frac{1}{3}(K_{IS}/K_{II}) \qquad (9)$$

$$\theta_n = 2\tan^{-1}\frac{1}{\sqrt{2}} \qquad (10)$$

The line to give the lower limiting value of ΔK_{II} for tensile mode growth, ΔK_{IIth} (tensile mode) in Fig. 3 has been obtained on the assumption that $\Delta K_{\sigma,max}$ given by the formular (5), (6), and (7) equals to 4.5kgf/mm$^{3/2}$ (1.4MPa·m$^{1/2}$), the lower limiting value for tensile mode growth in mode I loading given in Fig. 4. It is also noticed that da/dN in mode II growth is about ten times larger than da/dN in mode I growth which is shown by dash-dot-line in Fig. 4, if the comparison is made

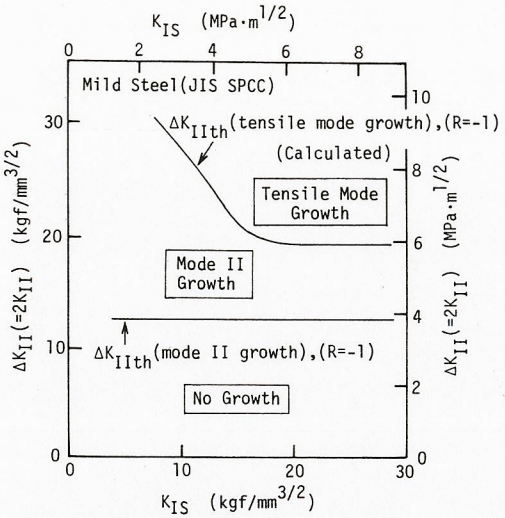

Fig. 9 Fatigue crack growth behavior under mode II loading in annealed mild steel (Otsuka, Mori, Ohshima, and Tsuyama, 1979).

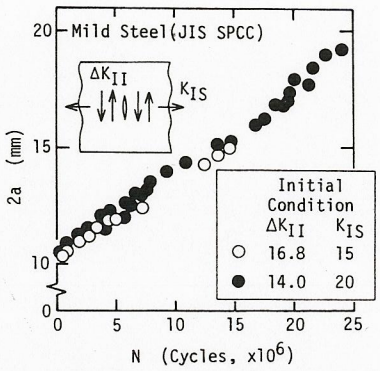

Fig. 10 Mode II crack growth curve of annealed mild steel.

at $\Delta K_I = \Delta K_{II}$. The dashed lines in Fig. 4 show the predicted da/dN in tensile mode growth under mode II loading for given K_{IS}. This curve was obtained in the similar way as explained above. Namely, putting $\Delta K_{\sigma,max} = \Delta K_I$ in the relations between $\Delta K_{\sigma,max}$ and (ΔK_{II}, K_{IS}) given by Eqs. (5), (6), and (7), and between ΔK_I and da/dN given by the dash-dot-line in Fig. 4, we obtain ΔK_{II} versus da/dN relation for given K_{IS} value. In Fig. 4, ΔK_{II} versus da/dN relations for K_{IS} = 0 and 20 are given. Figures 5 and 6 show macroscopic and microscopic views, respectively, of mode II fatigue crack growth.

2017-T4 : Figure 7 shows the fatigue crack growth behavior under mode II loading. It is noticed in this figure that ΔK_{IIth}(tensile mode) and ΔK_{IIth}(mode II) are very close. Therefore, fatigue crack growth under mode II loading occurs only in mode II in the region of larger ΔK_{II} than the threshold values shown in Fig. 7. In the region of smaller ΔK_{II} than these threshold no fatigue crack growth is observed. Figure 8 shows the ΔK_{II} versus da/dN relation. No effect of K_{IS} on ΔK_{II} versus da/dN relation is observed. It is seen in this case that da/dN for mode II growth is 7∼8 times larger than that for mode I growth which is shown by dash-dot-line in Fig. 8. Predicted da/dN for tensile mode growth under mode II loading obtained in the similar way as explained in Fig. 4 are shown by dashed lines in Fig. 8, where da/dN for tensile mode growth is lower than da/dN for mode II growth in almost all the region where a fatigue crack grows. This will be the reason why tensile mode growth is not observed under mode II loading in 2017-T4.

Mild steel : Figure 9 shows the fatigue crack growth behavior of annealed mild steel specimens under the combined ΔK_{II} and K_{IS} loading. The results show that if ΔK_{II} is larger than ΔK_{IIth}(tensile mode) shown by the upper curve in Fig. 9, a fatigue crack grows in the plane about 60° to the precrack, in which local tensile stress near the crack tip seems to be maximum, and if ΔK_{IIth}(mode II) < ΔK_{II} < ΔK_{IIth}(tensile mode), mode II growth occurs in the plane of precrack. If the K_{IS} is small, mode II

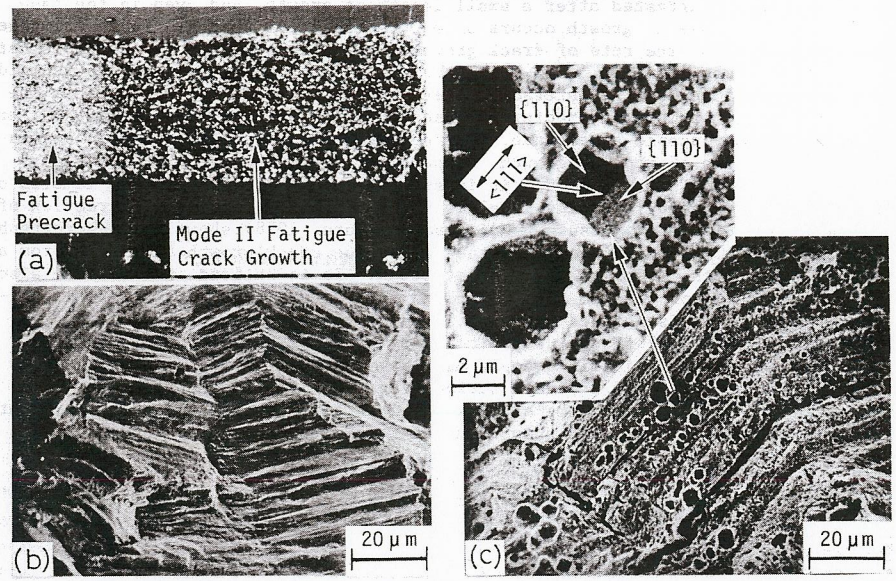

Fig. 11 Fracture surface of mode II fatigue crack growth in annealed mild steel.
(a) Macroscopic appearance of mode II fatigue crack growth
(b) SEM fractograph of mode II fatigue crack, ΔK_{II} = 17kgf/mm$^{3/2}$ (5.3 MPa·m$^{1/2}$), K_{IS} = 15kgf/mm$^{3/2}$ (4.7MPa·m$^{1/2}$), R = -1, da/dN = 3.5 x 10^{-7}mm/cycle
(c) Etch pits on the fracture surface of mode II fatigue crack growth, ΔK_{II} = 14.4kgf/mm$^{3/2}$ (4.5MPa·m$^{1/2}$), K_{IS} = 20kgf/mm$^{3/2}$ (6.2MPa·m$^{1/2}$), R = -1

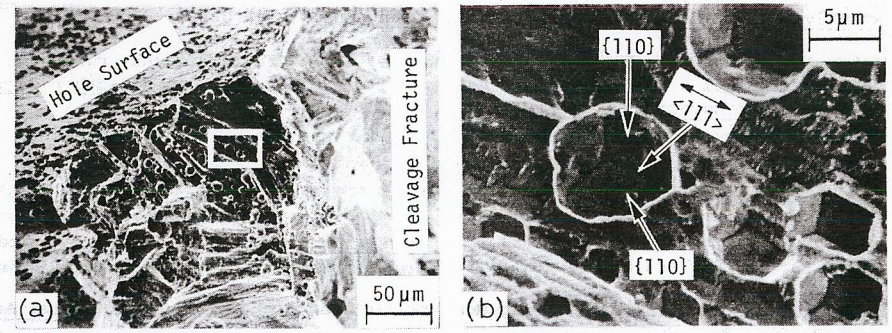

Fig. 12 Initial stage of the fatigue crack growth in 4mm diameter circular holed mild steel specimen. Observation was made after fracture in liquid nitrogen after off-loading at N = 8 x 10^5 (80%N_f). $\Delta\sigma$(range of nominal stress)=12.8kgf/mm^2 (126MPa), R = 0. Note the direction of the parallel lines in shear mode fatigue crack and the slip direction <111> which is shown in the etch pit.
(a) Fractograph of the initiation site of the fatigue crack
(b) A higher-magnification view of the area within the rectangle in (a)

growth is usually arrested after a small length of growth, and even in the case that continuous mode II growth occurs under the condition that K_{IS} is superimposed, the acceleration of the rate of crack growth with increase in crack length is hardly observed as shown in Fig. 10. These characteristics in mode II growth in mild steel will be caused by the interaction between the mating fracture surfaces due to the roughness of mode II fracture surface of mild steel. Figs. 11(a), (b), and (c) show the macroscopic appearance, SEM photograph, and crystallographic examination by etch pits of mode II growth, respectively. According to Fig. 11(c) (Otsuka, Mori, and Tsuyama, 1979), it is seen that the direction of the lamella or the line made by the neighboring lamellas is parallel to <111> , the direction of slip in iron. Figure 12 (Otsuka, Mori, and Kawamura, 1978) shows the fractographs of the initial stage, or stage I growth, in fatigue crack growth initiated from a circular hole in the specimen of the same steel. It is noticed in this case also that the direction of the lamellas of which the fracture surface consists is parallel to <111>. It is noticed in Figs. 11 and 12 that the fracture surfaces produced by mode II growth are very similar to those of stage I growth in SEM fractographs as well as in microscopic examinations by etch pits. These results suggest that both of these fracture surfaces are made of glide surfaces of iron known as pencil glide. The same steel with different heat treatment (annealed at 650°C. 1h. furnace cooled) has shown similar results to that explained above (Otsuka and co-workers, 1979). But in weldable structural steel (JIS SM50B), mode II growth is not seen (Otsuka and co-workers, 1979). In that case ΔK_{IIth} (tensile mode) means the lowest ΔK_{II} for fatigue crack growth.

REFERRENCES

Otsuka, A., K. Mori, and T. Miyata (1975), The condition of fatigue crack growth in mixed mode condition. Eng. Fract. Mech., 7, 429-439.

Otsuka, A., K. Mori, and T. Kawamura (1978), A fractographic investigation of fatigue crack initiation and initial growth in mild steel. J. Soc. Materials Science, Japan, 27, 49-53, (in Japanese).

Otsuka, A., K. Mori, and S. Tsuyama (1979), A fractographic investigation of the shear mode fatigue crack growth in mild steel by etch pits. Preprint of 2nd Fractography Symposium, Soc. Materials Science, Japan, 10-14, (in Japanese).

Otsuka, A., K. Mori, T. Ohshima, and S. Tsuyama (1979), Fatigue crack growth of steel and aluminum alloy specimens under mode II loading. Preprint of 13th Fatigue Symposium, Soc. Materials Science, Japan, 15-19, (in Japanese).

Pook, L. P. (1977), An observation on mode II fatigue crack growth threshold behavior. Int. J. of Fracture, 13, 867-869.

Pook, L. P. and A. F. Greenan (1979), Fatigue crack growth in mild steel under combined loading. In C. W. Smith (Ed.), Fracture Mechanics, ASTM STP 677, American society for Testing and Materials, pp. 23-35.

Roberts, R. and J. J. Kibler (1971), Mode II fatigue crack propagation. Trans. ASME, Series D, 93, 671-680.

Yokobori, T., A. T. Yokobori, and A. Kamei (1977), Fatigue crack growth under mode II loading. Trans. Japan Soc. Mech. Engineers, 43, 4345-4352, (in Japanese).